

**APPARATUS FOR IMPROVING THE COLD STARTING  
CAPABILITY OF AN ELECTROCHEMICAL FUEL CELL**

**Cross-Reference to Related Application(s)**

This application is a continuation-in-part of U.S. Patent Application Serial No. 09/406,318, entitled "Methods for Improving the Cold Starting  
5 Capability of an Electrochemical Fuel Cell". The '318 application is, in turn, a continuation-in-part of U.S. Patent Application Serial No. 09/138,625 filed August 24, 1998, entitled "Method and Apparatus for Commencing Operation of a Fuel  
10 Cell Electric Power Generation System Below the Freezing Temperature of Water". The '625 application is, in turn, a continuation of U.S. Patent Application Serial No. 08/659,921 filed June 7, 1996, now U.S. Patent No. 5,798,186 issued  
15 August 25, 1998, also entitled "Method and Apparatus for Commencing Operation of a Fuel Cell Electric Power Generation System Below the Freezing Temperature of Water". The '318, '625 and '921 applications are each hereby incorporated  
20 by reference in their entirety.

**Field Of The Invention**

The present invention relates to techniques to improve the cold start capability of an  
25 electrochemical fuel cell. More particularly, the present invention relates to apparatus for improving the cold start capability of fuel cell

electric power generation systems that include a solid polymer fuel cell stack.

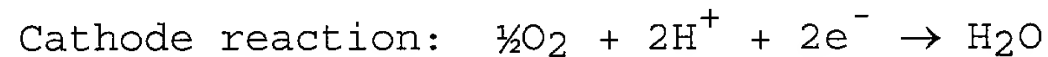
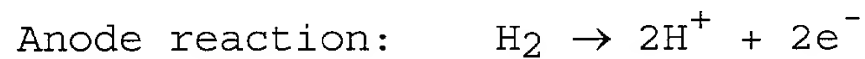
### Background Of The Invention

5           Electrochemical fuel cells convert fuel and oxidant to electricity and reaction product. Solid polymer electrochemical fuel cells generally employ a membrane electrode assembly ("MEA"), which comprises an ion exchange membrane or solid  
10   polymer electrolyte disposed between two electrodes typically comprising a layer of porous, electrically conductive sheet material, such as carbon fiber paper or carbon cloth. The MEA contains a layer of catalyst, typically in the  
15   form of finely comminuted platinum, at each membrane/electrode interface to induce the desired electrochemical reaction. In operation the electrodes are electrically coupled to provide a circuit for conducting electrons between the  
20   electrodes through an external circuit.

          At the anode, the fuel stream moves through the porous anode substrate and is oxidized at the anode electrocatalyst layer. At the cathode, the oxidant stream moves through the porous cathode  
25   substrate and is reduced at the cathode electrocatalyst layer to form a reaction product.

          In fuel cells employing hydrogen as the fuel and oxygen-containing air (or substantially pure oxygen) as the oxidant, the catalyzed reaction at  
30   the anode produces hydrogen cations (protons) from the fuel supply. The ion exchange membrane

facilitates the migration of protons from the anode to the cathode. In addition to conducting protons, the membrane isolates the hydrogen-containing fuel stream from the oxygen-containing oxidant stream. At the cathode electrocatalyst layer, oxygen reacts with the protons that have crossed the membrane to form water as the reaction product. The anode and cathode reactions in hydrogen/oxygen fuel cells are shown in the following equations:



In typical fuel cells, the MEA is disposed between two electrically conductive fluid flow field plates or separator plates. Fluid flow field plates have at least one flow passage formed in at least one of the major planar surfaces thereof. The flow passages direct the fuel and oxidant to the respective electrodes, namely, the anode on the fuel side and the cathode on the oxidant side. The fluid flow field plates act as current collectors, provide support for the electrodes, provide access channels for the fuel and oxidant to the respective anode and cathode surfaces, and provide channels for the removal of reaction products, such as water, formed during operation of the cell. Separator plates typically do not have flow passages formed in the surfaces thereof, but are used in combination with an

adjacent layer of material which provides access passages for the fuel and oxidant to the respective anode and cathode electrocatalyst, and provides passages for the removal of reaction products. The preferred operating temperature range for solid polymer fuel cells is typically 50°C to 120°C, most typically about 75°C to 85°C.

Two or more fuel cells can be electrically connected together in series to increase the overall power output of the assembly. In series arrangements, one side of a given fluid flow field or separator plate can serve as an anode plate for one cell and the other side of the fluid flow field or separator plate can serve as the cathode plate for the adjacent cell. Such a multiple fuel cell arrangement is referred to as a fuel cell stack, and is usually held together in its assembled state by tie rods and end plates. The stack typically includes inlet ports and manifolds for directing the fluid fuel stream (such as substantially pure hydrogen, methanol reformat or natural gas reformat, or a methanol-containing stream in a direct methanol fuel cell) and the fluid oxidant stream (such as substantially pure oxygen, oxygen-containing air or oxygen in a carrier gas such as nitrogen) to the individual fuel cell reactant flow passages. The stack also commonly includes an inlet port and manifold for directing a coolant fluid stream, typically water, to interior passages within the stack to absorb heat generated by the fuel cell during operation.

The stack also generally includes exhaust manifolds and outlet ports for expelling the depleted reactant streams and the reaction products such as water, as well as an exhaust manifold and outlet port for the coolant stream exiting the stack. In a power generation system various fuel, oxidant and coolant conduits carry these fluid streams to and from the fuel cell stack.

10        When an electrical load (comprising one or more load elements) is placed in an electrical circuit connecting the electrodes, the fuel and oxidant are consumed in direct proportion to the electrical current drawn by the load, which will  
15        vary with the ohmic resistance of the load.

      Solid polymer fuel cells generally employ perfluorosulfonic ion exchange membranes, such as those sold by DuPont under its NAFION trade designation and by Dow under the trade designation  
20        XUS 13204.10. When employing such membranes, the fuel and oxidant reactant streams are typically humidified before they are introduced to solid polymer fuel cells so as to facilitate proton transport through the ion exchange membrane and to  
25        avoid drying (and damaging) the membrane separating the anode and cathode of each cell.

      Each reactant stream exiting the fuel cell stack generally contains water. The outlet fuel stream from the anodes generally contains the  
30        water added to humidify the incoming fuel stream plus any product water drawn across the membrane

from the cathode. The outlet oxidant stream from the cathodes generally contains the water added to humidify the incoming oxidant stream plus product water formed at the cathode.

5           In some fuel cell applications, such as, for example, motive applications, it may be necessary or desirable to commence operation of a solid polymer electrolyte fuel cell stack when the stack core temperature is below the freezing temperature  
10 of water. As used herein, the freezing temperature of water means the freezing temperature of free water, that is, 0°C at 1 atmosphere. It may also be necessary or desirable when ceasing operation of the solid polymer fuel  
15 cell stack to improve the cold start capability and freeze tolerance of the stack by reducing the amount of water remaining within the fuel, oxidant and coolant passages of the stack. Upon freezing, water remaining within stack passages will expand  
20 and potentially damage structures within the stack such as, for example, the membrane/electrocatalyst interface, the reactant passageways, conduits and seals, as well as the porous electrode substrate material.

25           If there is an expectation that a solid polymer fuel cell stack will be subjected to cold temperatures, especially temperatures below the freezing temperature of water, one or more special start-up and shutdown techniques and associated  
30 apparatus may be used. These techniques may improve the cold start capability and freeze

tolerance of the stack, and improve the subsequent fuel cell performance. A measure of electrochemical fuel cell performance is the voltage output from the cell for a given current density. Higher performance is associated with a higher voltage output for a given current density or higher current density for a given voltage output.

10 **Summary Of The Invention**

According to one aspect of the invention, an electric power generation system is provided that includes a fuel cell stack connectable to an external electrical circuit; when so connected, the stack may supply electric current to the external circuit. The stack comprises at least one solid polymer fuel cell and fluid stream passages for directing fluid streams through at least one of the fuel cells. The system also includes a purge system that has a purge conduit having an inlet end connectable to a purge fluid supply, and an outlet end connectable to at least one of the fluid stream passages. The purge system also has a purge flow control device that controls the flow of a pressurized purge fluid through the purge conduit such that water can be purged from at least one of the fluid stream passages after a supply of electric current from the stack to the external circuit has been interrupted. The purge system is operable to improve the cold start capability and freeze

tolerance of its fuel cell stacks by reducing the amount of water remaining within the passages of the stack prior to stack freezing.

The fluid stream passages of the stack  
5 include passages for oxidant and fuel reactant streams. Any or all of the oxidant and fuel stream passages can be connected to the purge conduit upstream of the stack, so that purge fluid can be directed to one or both of the oxidant and fuel  
10 passages and through the fuel cell(s).

Additionally, a coolant passage may be connected to the purge conduit upstream of the stack to enable purge fluid to be transmitted therethrough.

The purge flow control device controls the  
15 purge operation during stack shut-down. A suitable purge flow control device includes a control valve connected to the purge conduit, and a control unit that is communicative with at least the control valve and optionally with one or more  
20 additional devices and sensors. In one aspect, the control unit is a microcontroller that is responsive to one or more input signals, and can control one or more devices. Upon receipt of an input signal to shut down the stack, the  
25 microcontroller opens a switch connecting the stack to the external circuit, thereby interrupting the supply of current from the stack to the circuit. Then, the control unit shuts off the reactant flow and opens the purge control  
30 valve for a selected period of time.



The purge system may further include a pressure regulator connected to the purge conduit and communicative with the control unit, to enable regulation of the pressure of purge fluid supplied to at least one of the reactant passages.

A suitable purge fluid is an inert gas, such as nitrogen. "Inert" in this sense means a fluid that is substantially non-reactive in the fuel cell.

According to another aspect of the invention, an electric power generation system is provided that has a humidifier bypass system. Such an electric power generation system comprises a fuel cell stack connectable to an external electrical circuit; when connected, the stack may supply electric current to the external circuit. The stack comprises at least one solid polymer fuel cell, reactant stream passages for directing reactant streams through at least one of the fuel cells, a humidifier in fluid communication with at least one of the reactant stream passages for humidifying a reactant stream supplied to the fuel cell stack, and a humidifier bypass system. The humidifier bypass system comprises at least one bypass conduit for transmitting at least one reactant from a reactant supply to the stack in fluid isolation from the humidifier, and a bypass control device for selectively directing flow of the reactant streams to the fuel cell stack through the humidifier or the humidifier bypass conduit.

Each bypass conduit typically includes an inlet end that is connected to one of the reactant stream passages upstream of the humidifier or directly to one of the reactant supplies, and an outlet end that is connected to one of the reactant stream inlet passages downstream of said humidifier and upstream of the stack.

The control device is operable to direct reactant fluid through the humidifier and to the stack during normal operation, that is, while electrical power is being generated by the stack, and through the bypass conduit and to the stack during a shut down procedure (for example, after supply of electric current from the stack to the external circuit has been interrupted). The control device may include at least one bypass inlet valve connected to one of the reactant passages upstream of the humidifier, and at least one bypass outlet valve connected to the same reactant passage downstream of the humidifier. The bypass conduit connects the bypass inlet and outlet valves so that reactant fluid can be transmitted in fluid isolation from the humidifier directly to the stack. The bypass control device preferably further includes a control unit communicative with the bypass inlet and outlet valves and with an input signal source. The control unit may be a micro-controller or other similar device.

**Brief Description Of The Drawings**

FIG. 1 is an exploded side view of a typical solid polymer electrochemical fuel cell with a  
5 membrane electrode assembly interposed between two fluid flow field plates.

FIG. 2 is a perspective cut-away view of an electrochemical fuel cell stack.

FIG. 3 is a schematic diagram of a fuel cell  
10 electric power generation system incorporating a nitrogen gas purge system.

FIG. 4 is a schematic diagram of a fuel cell electric power generation system incorporating a humidifier bypass purge system.

15 FIG. 5 is a composite plot of fuel cell stack voltage versus time in minutes (plot A) and fuel cell stack core temperature versus time in minutes (plot B) for a 10-cell stack, operation of which was commenced after the stack had equilibrated at  
20 a core temperature of  $-11^{\circ}\text{C}$ .

FIG. 6 is a composite plot of fuel cell stack voltage versus time in minutes (plot C) and fuel cell stack core temperature versus time in minutes (plot D) for a 4 cell stack, operation of which  
25 was commenced at a core temperature of  $-19^{\circ}\text{C}$ .

FIG. 7 is a plot of voltage as a function of current density for a fuel cell containing a membrane electrode assembly with a DowPont<sup>TM</sup> membrane exposed to three cold purge freeze/thaw  
30 cycles.

FIG. 8 is a plot of voltage as a function of current density for the fuel cell containing a membrane electrode assembly with a Nafion<sup>®</sup> 1135 membrane exposed to three cold purge freeze/thaw cycles.

FIG. 9 is a plot of voltage as a function of current density for a fuel cell containing a membrane electrode assembly with a Nafion<sup>®</sup> 1135 membrane exposed to one shorter duration cold purge freeze/thaw cycle.

FIG. 10 is a plot of voltage as a function of current density for a fuel cell containing a membrane electrode assembly with a DowPont<sup>™</sup> membrane exposed to three hot purge freeze/thaw cycles.

FIG. 11 is a plot of voltage as a function of current density for the fuel cell containing a membrane electrode assembly with a Nafion<sup>®</sup> 1135 membrane exposed to three hot purge freeze/thaw cycles.

FIG. 12 is a plot of cell voltage, for the fuel cell containing a membrane electrode assembly with a Nafion<sup>®</sup> 112 membrane, after each of a series of 55 cold purge freeze/thaw cycles.

FIG. 13 is a plot of stack voltage against operating time for an 8-cell Ballard Mark 513 fuel cell stack which was subjected to a series of freeze-thaw-operation cycles, interspersed with four heat treatment cycles.

FIG. 14 is a plot of stack voltage against current density for the fuel cell stack used to

generate the data of FIG. 12, before and after heat treatment

### Detailed Description Of The Preferred Embodiments

5           FIG. 1 illustrates a typical fuel cell 10. Fuel cell 10 includes a membrane electrode assembly 12 interposed between anode flow field plate 14 and cathode flow field plate 16. Membrane electrode assembly 12 consists of an ion  
10   exchange membrane 20 interposed between two electrodes, namely, anode 21 and cathode 22. In conventional fuel cells, anode 21 and cathode 22 comprise a substrate of porous electrically  
15   conductive sheet material 23 and 24, respectively, for example, carbon fiber paper or carbon cloth. Each substrate has a thin layer of electrocatalyst 25 and 26, respectively, disposed on one surface thereof at the interface with membrane 20 to render each electrode electrochemically active.  
20           As further shown in FIG. 1, anode flow field plate 14 has at least one fuel flow channel 14a formed in its surface facing anode 21. Similarly, cathode separator plate 16 has at least one  
25   oxidant flow channel 16a formed in its surface facing cathode 22. When assembled against the cooperating surfaces of electrodes 21 and 22, channels 14a and 16a form the reactant flow field passages for the fuel and oxidant, respectively. The flow field plates are electrically conductive.  
30           Turning now to FIG. 2, a fuel cell stack 100 includes a plurality of fuel cell assemblies, a

series of which is designated as 111 in FIG. 2.

Each of the fuel cell assemblies includes a membrane electrode assembly 112 interposed between a pair of fluid flow field plates 114, 116. Fuel  
5 cell stack 100 also includes a first end plate 130 and a second end plate 140.

Plate 130 includes fluid inlet ports 132, 134, 136 for introducing fluid fuel, oxidant and coolant streams, respectively, to the stack.

10 Plate 140 includes fluid outlet ports 142, 144, 146 for exhausting fluid fuel, oxidant and coolant streams, respectively, from the stack. The fluid outlet ports are fluidly connected to the corresponding fluid inlet ports via passages  
15 within the stack.

The fuel cell assemblies have a series of openings formed therein, which cooperate with corresponding openings in adjacent assemblies to form fluid manifolds 152, 154, 156, 162, 164, 166  
20 within the stack 100. The fluid manifolds are each circumscribed by a sealant material or gasket. In addition, a peripheral seal at the exterior perimeter of each fuel cell fluidly isolates the interior, electrochemically active  
25 portion of the fuel cell from the external environment.

A fuel stream entering the stack via fuel inlet port 132 is directed to the individual fuel flow field plates via manifold 152. After passing  
30 through the fuel flow field plate channels, the fuel stream is collected in manifold 162 and

exhausted from the stack via fuel outlet port 142. Similarly, an oxidant stream entering the stack via oxidant inlet port 134 is directed to individual oxidant flow field plates via manifold  
5 154. After passing through the oxidant flow field plate channels, the oxidant stream is collected in manifold 164 and exhausted from the stack via oxidant outlet port 144. A fluid coolant (typically water) introduced via coolant inlet  
10 port 136 is directed to coolant plate assemblies (not shown) in the stack 100 via manifold 156. The coolant stream is collected in manifold 166 and exhausted from the stack via coolant outlet port 146. Coolant manifolds 156, 166 may be fitted  
15 with a compliant mechanism (not shown), such as tube cushions or inserts made of closed cell foam, to accommodate the expansion of freezing water. Tie rods 170 extend between end plates 130 and 140 to compress and secure stack 100 in its assembled  
20 state with fastening nuts 172 disposed at opposite ends of each tie rod, and disc springs 174 interposed between the fastening nuts 172 and end plates 130, 140.

FIG. 3 is a schematic diagram of a fuel cell  
25 electric power generation system 200 comprising a fuel cell stack 210 and a nitrogen gas purge system 250. The fuel cell stack 210 includes negative and positive bus plates 212, 214, respectively, to which an external circuit  
30 comprising a variable load 216 is electrically connectable to the stack 210 by closing switch

218. The system includes a fuel (hydrogen) circuit, an oxidant (air) circuit, and a coolant water circuit. The reactant and coolant streams are circulated in the system 200 in various  
5 conduits illustrated schematically in FIG. 3.

A hydrogen supply 220 is connected to the stack 210; hydrogen pressure is controllable by pressure regulator 221. Water in the hydrogen stream exiting the stack 210 is accumulated in a  
10 knock drum 222, which can be drained by opening valve 223. Unreacted hydrogen is recirculated to stack 210 by a pump 224 in recirculation loop 225. An air supply 230 is connected to the stack 210, the pressure of which is controllable by pressure  
15 regulator 231. Water in the air stream exiting the stack 210 is accumulated in reservoir 232, which can be drained by opening valve 233, and the air stream is vented from the system via valve 234.

20 In the coolant water loop 240, water is pumped from reservoir 232 and circulated through stack 210 by pump 241. The temperature of the water is adjusted in a heat exchanger 242.

Purge system 250 is used to purge the  
25 hydrogen and oxidant passages in fuel cell stack 210 with a low humidity, non-reactive gas such as nitrogen. Flow of purge gas from a purge gas supply 260 to the hydrogen and air inlet passages 261, 262 is transmitted through purge supply  
30 conduits 268, 269 and three way valves 266, 267 connected to respective hydrogen and air inlet



passages 261, 262 upstream of the stack 210. The flow of nitrogen through each purge conduit 268, 269 is controlled by respective flow regulating valves 263, 264.

5        A micro-controller (not shown) or similar electronic control unit may be provided to automate at least some of the purge system operation. In a simple set-up, the micro-controller is programmed to control valves 221,  
10    231, 263, 264, 265 266, 267, and switch 218. Upon receipt of instructions to shut down the system, the micro-controller opens switch 218 to interrupt the flow of electricity from the stack 210 to the circuit, then closes air and hydrogen supply  
15    valves 221, 231 and opens valves 263, 264, 266, 267 to enable purge fluid to be transmitted through conduits 268, 269 to air and hydrogen conduits 261, 262 and through the stack 210.

20        An additional purge conduit and three way valve (both not shown) may be connected to the coolant loop upstream of the stack 210 to enable purging of the coolant loop during the shut down procedure. The micro-controller is adapted accordingly to shut down pump 241 and heat  
25    exchanger 242 prior to directing purge fluid to the coolant loop.

30        Alternatively, the reactant streams themselves can be employed as the purge streams. Preferably the purge fluid, if it is a gas, is dry or at least not humidified. Thus, when employing the reactant streams as the purge streams,

reactant stream humidifiers (if any) are bypassed to provide streams having water carrying capacity greater than humidified reactant streams.

Referring to FIG. 4, a humidifier bypass purge

5 system 300 replaces the nitrogen gas purge system 250 and comprises a series of valves and conduits that cooperate to direct the supply oxidant and fuel streams in fluid isolation from a humidifier. Particularly, upstream three-way bypass valves  
10 302, 304 are provided on respective fuel and oxidant inlet passages 261, 262 between the oxidant and fuel supply sources 220, 230, and a humidifier 306. The humidifier 306 is preferably a contact-type gas humidifier; however other types  
15 of humidifiers known to a person skilled in the art can be used, for example, a membrane humidifier. A fuel bypass conduit 308 is connected to upstream fuel bypass valve 302 and to a downstream three-way valve 267 connected to fuel  
20 inlet passage 261 downstream of humidifier 306 and upstream of stack 210. Similarly, an oxidant bypass conduit 310 is connected to upstream oxidant bypass valve 304 and to a downstream three-way valve 266 connected to the oxidant inlet  
25 passage 262 downstream of the humidifier 306 and upstream of stack 210. The respective oxidant and fuel upstream and downstream bypass valves 302, 304, 267, 266 are operated to direct reactant flow through humidifier 306 and to stack 210 during  
30 normal stack operation, and through bypass conduits 308, 310 to stack 210 during a purging

operation. As the bypass conduits 308, 310 are in fluid isolation from the humidifier 306, reactant supplied to the stack 210 via the bypass conduits 308, 310 avoid humidification. A control device  
5 (not shown ) similar to that used to control the purge system 250 may be programmed to control the humidification bypass operation.

FIG. 5 is a composite plot of fuel cell stack voltage versus time in minutes (plot A) and fuel  
10 cell stack core temperature versus time in minutes (plot B) for a 10-cell stack to which the flow of fuel and oxidant was restored after the stack had equilibrated at a core temperature of  $-11^{\circ}\text{C}$ .

The stack had been operating previously, and  
15 therefore the reactant flow passages contained moist gases. Before decreasing the stack core temperature below the freezing temperature of water, the reactant and coolant water passages within the stack were purged by circulating dry,  
20 compressed air through them. The stack core temperature was then lowered below the freezing temperature of water by exposing the stack to a surrounding environment with a temperature below the freezing temperature of water. For the  
25 purposes of the examples described herein, the stack was typically placed in an insulated chamber, with the fluid and electrical connections to the stack fitted through the chamber walls. Cold nitrogen gas from a liquid nitrogen source  
30 was circulated through the chamber. The stack core temperature was measured using a thermocouple

positioned in a thermally conductive plate located between two fuel cells in the center of the stack. Stack voltage, stack current and ambient temperature were also monitored.

5           When circulation of hydrogen and air through the stack was commenced at a stack core temperature of  $-11^{\circ}\text{C}$  (at time = 0 minutes), the open circuit voltage was normal. A load (360 amp) was connected in the circuit after approximately  
10 three minutes, causing the stack core temperature to rise rapidly while the voltage decreased but recovered gradually. Once operation of the stack had commenced, the exothermic reaction of hydrogen and oxygen within the stack and the resistive  
15 heating due to internal ohmic losses caused the stack core temperature to rise.

FIG. 6 is a composite plot of fuel cell stack voltage versus time in minutes (plot C) and fuel cell stack core temperature versus time in minutes  
20 (plot D) for a 4-cell stack, operation of which was commenced at a core temperature of  $-19^{\circ}\text{C}$ .

Again, as the stack had been operating previously, before decreasing the stack core temperature to  $-19^{\circ}\text{C}$ , the reactant passages within  
25 the stack were purged by circulating dry nitrogen. Coolant water remained in the coolant passages. Preferably the purge fluid is an inert gas such as nitrogen. Circulation of hydrogen and air was commenced with a load (50 amp) connected.  
30 Approximately 2 minutes transpired before the output current reached 50 amps. The load was

increased to 260 amps once the stack reached about 30°C, and the coolant pump was then activated. One cell in the stack was not operating properly; hence the lower than normal average cell voltages.

5        During commencement of stack operation, it has been found advantageous to refrain from circulating the fluid coolant stream within the stack until the stack has reached a temperature above the freezing temperature of water. More  
10        preferably, the fluid coolant stream is not circulated until the stack has reached a temperature at or near the desired stack operating temperature. In this regard, the circulating fluid coolant stream, assuming it is not pre-  
15        heated, will absorb and carry away heat otherwise available to warm the stack. Refraining from circulating the fluid coolant stream therefore expedites the warming of the stack to its desired operating temperature.

20        The cold start capability and freeze tolerance of fuel cells can be improved by reducing the amount of water remaining within the passages of the stack upon cessation of operation and reduction of stack core temperature to near or  
25        below the freezing temperature of water. As used herein, "freeze tolerance" refers to the ability of a fuel cell or fuel cell stack to maintain substantially the same performance after one or more freeze/thaw cycles.

30        The reactant passages, including the manifolds and individual fuel cell reactant flow

passages within a fuel cell stack, are preferably purged with a fluid stream before the temperature of the stack is decreased to below the freezing temperature of water. Preferably a fluid which is not reactive in the fuel cell environment, such as nitrogen gas, is used. A liquid may be used as the purge fluid. Preferably it would be a liquid that does not freeze at the temperature to which the fuel cell is to be exposed, and which has no detrimental effect on the fuel cell components.

The greater water carrying capacity of unhumidified reactant purge streams will result in more effective absorption and removal of water from the reactant stream conduits and porous components of the stack. Although all the reactant and coolant passages may be desirably purged in some situations, it has also been found effective in many cases to purge the oxidant stream passages only. This can simplify the system and the shutdown sequence.

It has been found that improved cold start capability and freeze tolerance of fuel cells to multiple freeze/thaw cycles can also be achieved when one or more of the fuel, oxidant, coolant and humidification passages are purged after the stack core temperature has been reduced to at or below normal room temperature (hereinafter referred to as "cold purging"). The beneficial effect of purging is not quite so pronounced when the stack passages are purged at a temperature within the

normal stack operating temperature range  
(hereinafter referred to as "hot purging").

#### EXAMPLES - PURGE METHODS

5

##### Experimental Details

The effect of cold and hot purging on  
membrane electrode assemblies having two different  
membrane types, Nafion<sup>®</sup> 1135 and a DowPont<sup>™</sup>  
10 membrane, in a Ballard Mark 513 single fuel cell  
with an internal humidifier was investigated.  
Separate water feed lines for the coolant and  
humidification streams were employed. The coolant  
outlet temperature was 85°C with a  $\Delta T$  (change in  
15 temperature from inlet to outlet) of 10°C at 1000  
amps per square foot (ASF) (10764 amps per square  
foot (ASM)), using air as the oxidant. Both MEAs  
had a screen printed anode containing 3.87 mg/cm<sup>2</sup>  
platinum black electrocatalyst on carbon fiber  
20 paper. For the cathode, both MEAs had 3.87 mg/cm<sup>2</sup>  
platinum black electrocatalyst applied by hand to  
carbon fiber paper. The Nafion<sup>®</sup> 1135 membrane  
employed in MEA No. 513-15 had an equivalent  
weight of 1100 and a thickness of about 85  $\mu\text{m}$   
25 (dry). The DowPont<sup>™</sup> membrane employed in MEA No.  
513-22 had an equivalent weight of 800 and a  
thickness of about 100  $\mu\text{m}$  (wet).

The Mark 513 cell was assembled and run  
overnight at 600 ASF (6458 ASM) at an air/fuel  
30 pressure of 30/30 psig (207/207 kPa gauge) and a

stoichiometry of 2/1.5 respectively. The fuel was substantially pure hydrogen. "Stoichiometry" is the ratio of the amount of reactant supplied to the fuel cell stack to the amount of reactant actually consumed in the fuel cell stack. In this instance, a fuel stoichiometry of 1.5 means that 150 parts of hydrogen are supplied to the fuel cell for each 100 parts actually consumed in the fuel cell.

10

#### Cold Purge Freeze/Thaw Cycles

For the initial series of three freeze/thaw cycles (results shown in FIGs. 7 and 8), the cell was cooled from its normal operating temperature (approximately 85°C) to room temperature (approximately 23°C) before purging. In each case, the fuel, oxidant, coolant and humidification passages were purged for approximately 7 minutes with nitrogen. The cell containing the Nafion<sup>®</sup> 1135 membrane was taken through a fourth freeze/thaw cycle with a purge duration of only approximately 1 minute (results shown in FIG. 8). The cell inlets and outlets were capped and the cell was placed in a freezer. Internal sealing pressure within the cell was maintained during freezing. The freezer temperature was approximately -20°C. The duration of the freeze ranged from 15-20 hours. After removal from the freezer, the coolant lines were connected and the cell was heated to 50°C. At that point, operation of the fuel cell was



commenced at 50 ASF (538.2 ASM) with excess fuel and oxidant flow rates. When the cell temperature reached 60°C, the current density was increased to 600 ASF (6458 ASM) and the cell was operated for  
5 at least one hour or until cell voltage had stabilized. A polarization test from 0 to 1000 ASF (0 to 10764 ASM) was performed for each of the two MEAs tested, using two different oxidant streams: air and substantially pure oxygen.

10 FIG. 7 is a plot of voltage as a function of current density for the fuel cell containing MEA 513-22 (DowPont<sup>TM</sup> membrane). Plots 1-4 show the performance on air prior to freezing (which is the plot with the solid line and solid data points  
15 ♦), and after each of the three cold purge freeze/thaw cycles described above. Plots 5-8 show the performance on oxygen prior to freezing (which is the plot with the solid line and solid data points ▲), and after each of the three cold  
20 purge freeze/thaw cycles described above. For each of the oxidant streams, the four plots in FIG. 7 are difficult to distinguish from one another.

FIG. 8 is a plot of voltage as a function of  
25 current density for the fuel cell containing MEA 513-12 (Nafion<sup>®</sup> 1135 membrane). Plots 1-4 show the performance on air prior to freezing (which is the plot with the solid line and solid data points  
♦), and after each of the three cold purge  
30 freeze/thaw cycles described above. Plots 5-8 show the performance on oxygen prior to freezing

(which is the plot with the solid line and solid data points ▲), and after each of the three cold purge freeze/thaw cycles described above. Again, for each of the oxidant streams, the four plots in  
5 FIG. 8 are difficult to distinguish from one another.

FIG. 9 is a plot of voltage as a function of current density for the fuel cell containing MEA 513-12 (Nafion® 1135 membrane). Plots 1-2 show  
10 the performance on air prior to freezing (which is the plot with the solid line and solid data points ♦), and after the fourth cold purge freeze/thaw cycle described above, in which a shorter purge duration (approximately 1 minute) was used. Plots  
15 3-4 show the performance on oxygen prior to freezing (which is the plot with the solid line and solid data points ▲), and after the fourth cold purge freeze/thaw cycle described above. Again, for each of the oxidant streams, the two  
20 plots in FIG. [8] 9 are difficult to distinguish from one another, indicating that a shorter duration purge can give satisfactory results.

Thus, based on the results shown in FIGs. 7, 8 and 9 for both MEAs, substantially no mass  
25 transport losses were exhibited over the series of three or four freeze/thaw cycles. The performance after each freeze/thaw cycle was maintained at approximately baseline (prior to freezing) polarization levels. Both MEAs thus exhibited  
30 favorable freeze/thaw tolerance when the cold purging technique was used.

### Hot Purge Freeze/Thaw Cycles

For a subsequent series of three freeze/thaw cycles, each cell was purged at stack operating temperature (approximately 85°C) before cooling.

5 The fuel, oxidant, coolant and humidification passages were purged for approximately 1 minute with nitrogen. The cell inlets and outlets were capped and the cell was placed in a freezer. Internal sealing pressure within the cell was

10 maintained during freezing. The freezer temperature was approximately -20°C. The duration of the freeze ranged from 15-20 hours. After removal from the freezer, the coolant lines were connected and the cell was heated to operating

15 temperature and operation commenced using essentially the same procedure employed for the cold purge freeze/thaw cycles described above. A polarization test from 0 to 1000 ASF (0 to 10764 ASM) was performed for each of the two MEAs

20 tested, again using two different oxidant streams: air and substantially pure oxygen.

FIG. 10 is a plot of voltage as a function of current density for the fuel cell containing MEA 513-22 (DowPont<sup>TM</sup> membrane). Plots 1-4 show the

25 performance on air prior to freezing (which is the plot with the solid line and solid data points ♦), and after each of the three hot purge freeze/thaw cycles described above. Plots 5-8 show the performance on oxygen prior to freezing

30 (which is the plot with the solid line and solid data points ▲), and after each of the three hot

purge freeze/thaw cycles described above. A significant mass transport effect appears to occur at higher current densities on air after the third freeze cycle, based on the increased difference  
5 between the air and oxygen performance levels.

FIG. 11 is a plot of voltage as a function of current density for the fuel cell containing MEA 513-12 (Nafion<sup>®</sup> 1135 membrane. Plots 1-4 show the performance on air prior to freezing (which is the  
10 plot with the solid line and solid data points ♦), and after each of the three hot purge freeze/thaw cycles described above. Plots 5-8 show the performance on oxygen prior to freezing (which is the plot with the solid line and solid  
15 data points ▲), and after each of the three hot purge freeze/thaw cycles described above. Again, a significant mass transport effect appears to occur at higher current densities on air, based on the progressively increasing difference between  
20 the air and oxygen performance levels after each freeze/thaw cycle.

The particularly favorable results obtained with the cold purge technique were further supported by the following test in which a single  
25 fuel cell was cycled through 55 freeze/thaw cycles, with the purge technique used on the coolant and cathode side passages only.

#### Experimental Details

30 The effect of repeated cold purging on a membrane electrode assembly having a Nafion<sup>®</sup> 112

membrane, in a Ballard Mark 513 single fuel cell with an external humidifier was investigated. Separate water feed lines for the coolant and humidification streams were employed. The coolant  
5 inlet temperature was 70°C with a  $\Delta T$  (change in temperature from inlet to outlet) of 15°C at 1 A/cm<sup>2</sup> using air as the oxidant. The MEA had a screen printed anode containing 0.34-0.38 mg/cm<sup>2</sup> platinum black electrocatalyst and a screen  
10 printed cathode containing 0.73-0.82 mg/cm<sup>2</sup> platinum black electrocatalyst on carbon fiber paper, both with a Nafion spray coating (0.2 mg/cm<sup>2</sup>).

The cell was tested in a temperature-  
15 controlled environmental chamber at an air/fuel pressure of 27/27 psig (186/186 kPa gauge) and a stoichiometry of 1.8/1.2 respectively. The fuel was a simulated methanol reformat stream (composition 63.5% hydrogen; 22.5% carbon dioxide;  
20 13% nitrogen; 1% methanol and 40 parts per million (ppm) carbon monoxide), and a 4% air bleed was employed at the anode. The fuel and oxidant streams were humidified.

For the series of 55 freeze/thaw cycles  
25 (results shown in FIG. 12), the cell was cooled from its normal operating temperature (approximately 80°C) to a chamber temperature at which no part of the stack was below 0°C, but where the cell temperature was approximately 30°C  
30 before purging. In each case, the oxidant passages were purged for approximately 10 seconds

with dry (unhumidified) air. The cell inlets and outlets were closed by actuated valves, and the temperature in the chamber was reduced to approximately  $-25^{\circ}\text{C}$ . The duration of each freeze  
5 was approximately 1 hour. Internal sealing pressure within the cell was maintained during freezing. The cell was then thawed to  $5^{\circ}\text{C}$  and then heated, by circulating warm coolant, to  $65^{\circ}\text{C}$ . At that point, operation of the fuel cell was  
10 commenced at  $0.5\text{ A/cm}^2$  for 60 minutes, then at  $1.0\text{ A/cm}^2$  for 30 minutes, then for a second time at  $0.5\text{ A/cm}^2$  for 30 minutes.

FIG. 12 shows the results obtained after each of 55 such cycles with the cell voltage measured  
15 once it had stabilized at  $1.0\text{ A/cm}^2$  during the 30 minutes of operation at that current density (Plot A) and once it had stabilized at  $0.5\text{ A/cm}^2$  during the second period of operation at that current density (Plot B). At both current densities the  
20 performance degradation over the 55 cycles was negligible: approximately  $-0.1\text{ mV/cycle}$  at  $0.5\text{ A/cm}^2$  and approximately  $-0.2\text{ mV/cycle}$  at  $1.0\text{ A/cm}^2$ .

25

#### EXAMPLES - HEAT TREATMENT METHODS

FIG. 13 shows a plot of stack voltage against operating time for an 8-cell Ballard Mark 513 fuel cell stack which was subjected to a series of  
30 freeze-thaw-operation cycles. Prior to freezing the fuel, oxidant and coolant passages were purged

with dry gas. During the freezing cycles, the cell inlets and outlets were capped and the cell was placed in a freezer. Internal sealing pressure within the cell was maintained during freezing. The freezer temperature was approximately  $-20^{\circ}\text{C}$ . The duration of the freeze in each case was greater than 12 hours. After some cycles the stack was operated normally, and after other cycles the stack operating temperature was increased to above its normal operating temperature for a period, before normal operation was resumed. The stack was operated on humidified air and hydrogen, both at 30 psig (207 kPa gauge), at stoichiometries of 2.0 and 1.5 respectively, at a current density of 700 ASF (7535 ASM) to generate the data shown in FIG. 12. The coolant inlet temperature was  $75^{\circ}\text{C}$  with a  $\Delta T$  (change in temperature from inlet to outlet) of  $10^{\circ}\text{C}$  at 1000 ASF (10764 ASM).

Referring to FIG. 13, between 425 and 882 hours the stack was operated, frozen several times, and then started up having been warmed to  $50^{\circ}\text{C}$ . Data points obtained directly after a freeze cycle are marked "F". It can be seen that the cell performance deteriorated after each freeze cycle. After 882 hours the stack was started up after freeze cycles having been warmed to only  $10^{\circ}\text{C}$ . After 950 hours the stack was started up after freeze cycles having been warmed to only  $0^{\circ}\text{C}$ . The performance losses observed did

not appear to be significantly affected by the start temperature.

A substantial improvement in performance after freezing was obtained in 4 cases where stack operation was commenced and then the stack operating temperature was increased to above the normal stack operating temperature of about 85°C, namely, to approximately 100°C. Data points obtained directly after such heat treatments are marked "H".

FIG. 14 shows a plot of stack voltage as a function of current density for the 8-cell Ballard Mark 513 fuel cell stack used to generate the data of FIG. 13. Plots A, B and C show performance curves for operation on air, and plots D, E and F for operation on oxygen. Plots A and D show the stack performance before any of the heat treatments referred to the description of FIG. 13 but after the final freeze cycle, plots B and E show the stack performance immediately after the fourth heat treatment, and plots C and F show the stack performance about 2 days after the fourth heat treatment. The results on air show a substantial and sustained improvement in post-freezing performance after the heat treatment. The improvement is believed to be attributable to improved mass transport in the MEA, based on the fact that on oxygen the performance was not significantly affected by the heat treatment. This indicates that performance loss after freezing may be, at least in part, due to mass



transport difficulties in the cells, which have a more significant effect on air than on a substantially pure oxidant stream. These detrimental effects could be due to retained water  
5 in the membrane electrode assembly. It is possible that the heat treatment method assists in removing residual water from the membrane electrode assembly, and thereby improves performance at start-up, particularly on air.

10 While particular elements, embodiments and applications of the present invention have been shown and described, it will be understood, of course, that the invention is not limited thereto since modifications may be made by those skilled  
15 in the art without departing from the scope of the present disclosure, particularly in light of the foregoing teachings